Monomeric *S*-Adenosylmethionine Decarboxylase from Plants Provides an Alternative to Putrescine Stimulation[†,‡]

Eric M. Bennett,[§] Jennifer L. Ekstrom,[§] Anthony E. Pegg,[∥] and Steven E. Ealick*[,§]

Department of Chemistry and Chemical Biology, Cornell University, Ithaca, New York 14853-1301, and Departments of Cellular and Molecular Physiology and Pharmacology, Milton S. Hershey Medical Center, Pennsylvania State University College of Medicine, Hershey, Pennsylvania 17033

Received August 23, 2002; Revised Manuscript Received October 10, 2002

ABSTRACT: *S*-Adenosylmethionine decarboxylase has been implicated in cell growth and differentiation and is synthesized as a proenzyme, which undergoes autocatalytic cleavage to generate an active site pyruvoyl group. In mammals, *S*-adenosylmethionine decarboxylase is active as a dimer in which each protomer contains one α subunit and one β subunit. In many higher organisms, autocatalysis and decarboxylation are stimulated by putrescine, which binds in a buried site containing numerous negatively charged residues. In contrast, plant *S*-adenosylmethionine decarboxylases are fully active in the absence of putrescine, with rapid autocatalysis that is not stimulated by putrescine. We have determined the structure of the *S*-adenosylmethionine decarboxylase from potato, *Solanum tuberosum*, to 2.3 Å resolution. Unlike the previously determined human enzyme structure, the potato enzyme is a monomer in the crystal structure. Ultracentrifugation studies show that the potato enzyme is also a monomer under physiological conditions, with a weak self-association constant of 6.5×10^4 M^{-1} for the monomer−dimer association. Although the potato enzyme contains most of the buried charged residues that make up the putrescine binding site in the human enzyme, there is no evidence for a putrescine binding site in the potato enzyme. Instead, several amino acid substitutions, including Leu13/Arg18, Phe111/Arg114, Asp174/Val181, and Phe285/His294 (human/potato), provide side chains that mimic the role of putrescine in the human enzyme. In the potato enzyme, the positively charged residues form an extensive network of hydrogen bonds bridging a cluster of highly conserved negatively charged residues and the active site, including interactions with the catalytic residues Glu16 and His249. The results explain the constitutively high activity of plant *S*-adenosylmethionine decarboxylases in the absence of putrescine and are consistent with previously proposed models for how putrescine together with the buried, negatively charged site regulates enzyme activity.

S-Adenosylmethionine decarboxylase (AdoMetDC)[1] is an essential enzyme for the formation of polyamines, providing decarboxylated *S*-adenosylmethionine (dcAdoMet), which is used as an aminopropyl donor by spermidine and spermine synthases (*1*−*3*). Once decarboxylated, *S*-adenosylmethionine (AdoMet) is no longer available for use by methyltransferases and is therefore committed to polyamine biosynthesis. Eukaryotic AdoMetDCs have been isolated from many species, and all consist of two nonidentical α and β subunits. The N-terminus of the α subunit is covalently bound to a pyruvoyl group that acts to form a Schiff base with the AdoMet substrate, facilitating decarboxylation. The pyruvate is formed from an internal serine residue of the proenzyme by an autocatalytic rearrangement, forming an internal ester bond and cleaving this bond to form a terminal dehydroalanine, which is then hydrolyzed to form the pyruvate. A second result of autocatalysis is generation of the α subunit from the C-terminus of the proenzyme and the β subunit from the N-terminus (*4*−*6*). The proenzyme sequence [-(Tyr/Phe)(Val/Leu)(Ser/Thr)Glu**Ser**Ser(Leu/Met/Glu)(Phe/Met)-(Val/Phe)-] surrounding the serine is conserved in all eukaryotic AdoMetDC sequences (*7*−*10*).

Polyamines are essential metabolites in plants, and their biosynthesis, oxidation, conjugation, and roles in differentiation, development, and resistance to stress in plants have been studied extensively (reviewed in refs *11*−*13*). At least 30 AdoMetDC sequences from 17 species of higher plants have been identified, and several of these, including those from potato (*7*), periwinkle (*14*), carnation (*15*), and *Arabidopsis thaliana* (*16*), have been cloned, expressed, and studied in some detail. In general, the properties of these enzymes, such as substrate specificity, are quite similar to those of the mammalian AdoMetDCs, with the notable exception of the absence of putrescine activation described below.

[†] This work was supported by the National Cancer Institute of the National Institutes of Health (Grant CA-18138 to A.E.P.). S.E.E. is also indebted to the W. M. Keck Foundation and the Lucille P. Markey Charitable Trust.

[‡] The coordinates of the potato AdoMetDC structure have been deposited in the Protein Data Bank under accession number 1MHM.

* To whom correspondence should be addressed. Telephone: (607) 255-7961. Fax: (607) 255-1227. E-mail: see3@cornell.edu.

[§] Cornell University.

[∥] Pennsylvania State University College of Medicine.

[1] Abbreviations: AdoMetDC, *S*-adenosylmethionine decarboxylase; AdoMet, *S*-adenosylmethionine; dcAdoMet, decarboxylated *S*-adenosylmethionine; MAOEA, 5′-deoxy-5′-[*N*-methyl-*N*-[2-(aminooxy)ethyl]-amino]adenosine.

10.1021/bi026710u CCC: $22.00
Published on Web 11/14/2002

AdoMetDC plays a critical role in the regulation of the content of polyamines in response to internal and external stimuli, and its levels in mammals and plants are highly regulated at multiple points. These include mRNA translation, where the presence of a complex structure in the 5′-UTR, which includes a small ORF, has been implicated in changes of the rate of AdoMetDC synthesis (*17*, *18*). AdoMetDC activity is also regulated at the level of transcription. Substantial changes in mRNA content occur in response to polyamine content, growth factors, and other agents. In plants, the content of AdoMetDC mRNA and its protein is strikingly altered during development, senescence, and exposure to exogenous agents (*19*−*23*). Experiments using antisense approaches or inhibitors of AdoMetDC have shown that these changes are critical for normal development and resistance to altered environmental conditions (*22*, *24*−*26*). Thus, AdoMetDC is an important factor in plant survival.

Many AdoMetDCs, including those from mammals (*27*, *28*), nematodes (*29*, *30*), fungi (*9*), and protists (*31*), are activated by putrescine. In mammals activation occurs as both an increase in the rate of proenzyme processing and an increase in the rate of decarboxylation and is an important mechanism in polyamine regulation, which allows for the efficient coupling of the production of the two precursors of spermidine. Such coupling is likely to be less important in plants, in which putrescine is used not only for the synthesis of polyamines but also for the production of various conjugation products and secondary metabolites (*11*−*13*). Plant AdoMetDCs do not require putrescine for maximal activity, and studies of the plant AdoMetDC proenzyme show that processing occurs very rapidly without the need for any cofactors (*7*, *15*). It appears that the plant AdoMetDCs are constitutively maintained in an active form, permitting rapid proenzyme processing and optimal activity of the finished enzyme, but the mechanism of this constitutive activation has remained unclear.

In the human enzyme (*6*), structural analysis shows that a putrescine molecule is bound to the enzyme in an unusual cluster of buried, negatively charged residues located between the two β-sheets. Putrescine makes direct interactions with the side chains of Glu15, Asp174, and Thr176, as well as indirect, water-mediated interactions with the side chains of Glu15, Ser113, Glu178, and Glu256. Ekstrom et al. hypothesized that activation of both decarboxylation and proenzyme processing might occur either by propagation of hydrogen-bonding effects between this negatively charged site and the active site or by structural stabilization of the interactions between the clusters of negatively charged residues on the two β-sheets (*6*).

On the basis of a sequence alignment with the potato enzyme, both hypotheses can be considered for the potato enzyme as well. The potato sequence conserves all of the putrescine binding residues except Ser113, which is replaced by Thr, and Asp174, which is replaced by Val. The latter substitution suggests that the potato enzyme should be less responsive to putrescine than the human enzyme and, perhaps, less active as a result. However, as noted above, the biochemical data point to constitutive high activity, which might be the case if putrescine binding to the potato enzyme is so tight that putrescine is effectively impossible to remove. This would be consistent with the observation that putrescine was repeatedly observed bound to the human enzyme even when putrescine was not added during crystallization (*6*, *32*). The 2.3 Å resolution crystal structure of the potato enzyme described below leads to a different and unexpected explanation for the constitutively high activity and provides direct evidence that a hydrogen-bonding chain between the negatively charged site and the active site affects the autocatalytic processing reaction. In addition, the structure and ultracentrifugation results reveal that potato AdoMetDC does not, as had been previously assumed (*6*), adopt a dimeric quaternary structure.

Table 1: Summary of X-ray Diffraction Data Collection and Processing

wavelength (Å)	1.54
resolution (Å)	2.1
space group	$P2_12_12_1$
cell dimensions (Å)	
a	65.65
b	71.64
c	72.33
unique reflections[a]	17049 (1084)
completeness (%)[a]	90.1 (69.6)
redundancy[a]	3.8 (2.8)
R_{sym} (%)[a]	8.7 (31.8)
I/σ[a]	8.3 (2.9)

[a] Values in parentheses are for the highest resolution shell containing data used in the refinement, 2.37−2.26 Å.

EXPERIMENTAL PROCEDURES

Protein Expression and Crystallization. The potato AdoMetDC DNA was inserted into the pQE31 vector as previously described (*7*), replacing the three N-terminal residues MetGluMet with the sequence MetArgGlySer$(His)_6$ThrAspPro to facilitate purification by metal affinity chromatography. The vector was transformed into *Escherichia coli* strain JM109. Cells were grown in ZB media, and histidine-tagged enzyme was purified. Crystals of potato AdoMetDC grew at 17 °C in 2 + 2 μL hanging drops, with a well solution of 0.1 M trisodium citrate dihydrate (pH 5.6), 20% v/v 2-propanol, and 20% w/v PEG 4000. Crystals first appeared several months after setup. The high PEG concentration protected the crystals from damage during freezing, without the need for additional cryoprotection.

X-ray Intensity Measurement. Diffraction data were measured on a flash-frozen crystal measuring 0.2 mm × 0.2 mm × 0.3 mm, using Cu Kα X-rays from a Rigaku rotating anode generator (50 kV, 100 mA) and a MAR 30 cm image plate detector system. Data were measured using 1° oscillation frames and a 1200 s exposure time. An initial pass of 72° provided complete data to 2.45 Å resolution. An additional 50° of data was collected with a closer detector distance to improve the resolution. The data were indexed in space group $P2_12_12_1$ with unit cell dimensions $a = 65.7$ Å, $b = 71.6$ Å, and $c = 72.3$ Å and scaled to 2.1 Å resolution using the programs DENZO and SCALEPACK (*33*), with a resulting R_{merge} of 7.7%. Final data collection statistics are presented in Table 1.

Structure Solution and Refinement. Initial phases were obtained by molecular replacement, using all chain A protein atoms of the 1.5 Å resolution human H243A structure (PDB code 1JL0) as a search model (*6*). Rotation and translation searching were performed with the program CNS (*34*) using

Table 2: Summary of Refinement Statistics

resolution range (Å)	500−2.3
reflections	
working set[a]	13948 (1070)
test set[a]	710 (61)
R-factor (%)[a]	21.8 (28.9)
R_{free} (%)[a]	28.4 (39.8)
no. of protein atoms	2360
no. of water molecules	85
RMS deviations	
bonds (Å)	0.0060
bond angles (deg)	1.2
torsion angles (deg)	25
improper torsion angles (deg)	0.81
B-factors (Å^2, protein atoms only)	
minimum	13.4
maximum	77.9
average	37.6

[a] Values in parentheses are for the highest resolution shell.

data to 4 Å resolution. Refinement of the molecular replacement model was carried out at 2.3 Å resolution. Except for the final round of refinement, 4.5% of the data (710 reflections at 2.3 Å resolution) was set aside for cross-validation. Bulk solvent and overall anisotropic *B*-factor adjustments were applied during refinement.

The initial molecular replacement solution (*R*-factor 51%) was optimized by rigid body refinement and simulated annealing. A composite omit map showed some errors in the backbone placement and missing density for several loops. After manual adjustment of the backbone using the program O (*35*), the model was mutated to the potato sequence and refined by successive rounds of simulated annealing, manual rebuilding in O, energy minimization, and group *B*-factor refinement in CNS. Some missing regions of the protein appeared during this stage. When the *R*-factor reached 25.4% (30.2% R_{free}), few changes remained to be made in the protein. Water molecules were then added for $F_o - F_c$ map peaks above 3σ if the putative water molecule had possible hydrogen-bonding contacts and no bad van der Waals contacts. After further refinement, including individual *B*-factor refinement, the model converged to an *R*-factor of 21.8% (R_{free} 28.4%). Additional water picking failed to lower R_{free}, and the results were not included in the model. A final round of refinement using all reflections gave the finished model with an *R*-factor of 21.7%. Final refinement statistics are presented in Table 2.

Active Site Modeling. To construct a model for substrate binding in potato AdoMetDC, the program ProFit (*36*) was used to superimpose the crystal structure of the human AdoMetDC complex with bound ligand (*32*) on the potato structure. The compound 5′-deoxy-5′-[*N*-methyl-*N*-[2-(aminooxy)ethyl]amino]adenosine (MAOEA) was chosen because it is a suicide inhibitor with the same number of atoms as dcAdoMet. Residues 4−10 of subunit B of the human structure, corresponding to residues 9−15 of the potato structure, were attached to potato residue Glu16, and the MAOEA residue was attached to the pyruvoyl group of the potato enzyme. The resulting structure was energy minimized to a gradient of 0.05 kJ mol^{-1} Å^{-1} using the OPLS-AA force field (*37*), GB/SA solvation model (*38*), and TNCG minimizer (*39*) as implemented in version 7.2 of the program MacroModel (*40*). During minimization, hydrogen atoms and atoms derived from the human structure or Glu16 and the pyruvoyl group were unrestrained, while all other non-hydrogen atoms were frozen in place.

Sedimentation Equilibrium. Analytical ultracentrifugation was performed at 20 °C in a Beckman XL-A centrifuge equipped with absorbance optics using a four-hole AN60 Ti rotor, six-sector charcoal−epon centerpieces, and fused silica windows. Two concentrations of the AdoMetDC protein solution in 100 mM sodium citrate buffer, pH 6.0, with nominal optical densities of 0.15 and 0.30 were centrifuged simultaneously. Absorbance data at 280 nm were obtained at 15000, 20000 and 25000 rpm. Equilibrium was assumed to be reached when scans taken 12 h apart were completely superimposable. Five scans were averaged for each rotor speed. Analysis was carried out as described (*41*). Self-association models were tested using the program NONLIN (*42*). Six data sets were analyzed by the global least squares minimization algorithm where the association stoichiometry, *n*, and the association constant, K_n, were the parameters that were optimized. The values of K_n were obtained in absorbance units, which were converted to molar units using the value 39975 M^{-1} cm^{-1} for the molar extinction coefficient of potato AdoMetDC at 280 nm.

RESULTS

Quality of the Final Model. Potato AdoMetDC crystallizes in space group $P2_12_12_1$ with unit cell dimensions $a = 65.7$ Å, $b = 71.6$ Å, and $c = 72.3$ Å. The asymmetric unit contains one AdoMetDC monomer, consisting of one α subunit and one β subunit, and has a solvent content of 51%. The final model contains 2360 protein atoms (including the covalently attached pyruvoyl group) and 84 water molecules. The final $2F_o - F_c$ electron density map shows ambiguous or uninterpretable density for the missing residues 1−14, 30−33, 120−130, and 338−360 and for the side chains of residues 15, 131, 161, 162, 176, and 203, which are modeled as alanines. The coordinate error from the Luzzati plot (*43*) is 0.30 Å for the working set and 0.40 Å for the test set. Ramachandran plot (*44*) analysis with PROCHECK (*45*) shows 86.4% of the residues to be in the most favored region, 12.8% in additionally allowed regions, and two residues each (0.8%) in the generously allowed and disallowed regions. The residues (Thr162 and Glu204) in the disallowed region occur in the two loops with the highest *B*-factors observed in the structure. No density was observed for the Thr162 side chain, and small breaks in the backbone density at Glu204 are observed at 1σ in the final $2F_o - F_c$ map. The *R*-factor for the final model is 21.8% with an R_{free} of 28.4% (Table 2).

Overall Structure. Monomeric potato AdoMetDC adopts the same four-layer α/β fold as the dimeric human enzyme, with two central eight-strand β-sheets flanked on either side by a total of seven α- and four 3_{10}-helices (Figure 1). The larger, C-terminal α subunit contributes thirteen β-strands, six α-helices, and three 3_{10}-helices, with the remainder contributed by the β subunit. Residues 299−307, which correspond to the disordered region 290−298 in the human structures, include one of the α-helices. Each potato enzyme monomer is packed in the crystal with ten other monomers within 8 Å but makes direct hydrogen-bonding contacts with only six of these. In contrast, the human AdoMetDC forms dimers in the crystal structure. Analysis of potato AdoMetDC

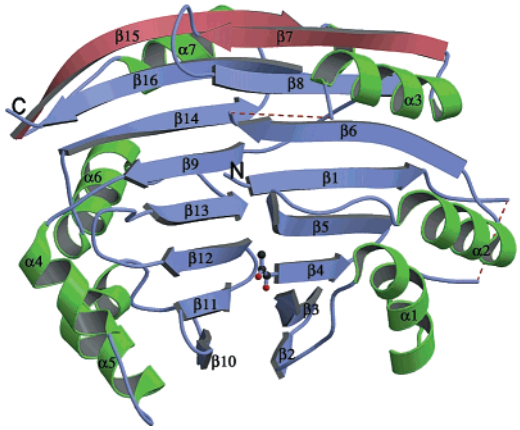

FIGURE 1: Potato AdoMetDC monomer. Potato AdoMetDC is a monomer, as observed in the crystal structure and as determined by ultracentrifugation (see text). The fold of the monomer is similar to the protomer of the human AdoMetDC dimer. β-Sheets are shown in blue (except the sheets analogous to the dimer interface in human AdoMetDC, shown in red), α-helices in green, and main chain breaks in dashed lines, and the active site pyruvoyl group is in ball-and-stick representation. This figure was prepared with Molscript (*54*) and Raster3D (*55*).

by ultracentrifugation carried out with the protein dissolved in 100 mM sodium citrate, pH 6.0, shows that the monomeric units self-associated only weakly with a K_{1-2} of 6.5×10^4 M^{-1}. This value reduces slightly to 6.2×10^4 M^{-1} when 0.5 M NaCl is included in the solution. These results show that potato AdoMetDC is also a monomer under physiological conditions.

Buried Charged Site. The structure of the buried charged site in the potato enzyme provides an unexpectedly striking contrast with that of the human enzyme. In human AdoMetDC a buried negatively charged site provides a binding site for a putrescine molecule (*32*). At the mouth of the binding site, putrescine is held in place by hydrogen bonds to the side chains of Asp174, Thr176, and Glu15 (Figure 2A). The other putrescine amino group, at the back of the binding site, has indirect interactions with Glu15, Ser113, Glu178, and Glu256 mediated by three water molecules. The phenyl rings of Phe111 and Phe285 pack against the hydrophobic center of the bound putrescine molecule. A chain of hydrogen bonds stretches from putrescine through the three water molecules and Glu256 to Lys80, a fourth water molecule, Ser254, and finally to Glu11 in the active site.

By contrast, no putrescine is observed in the charged site of potato AdoMetDC, nor does the site contain enough available room to allow such binding (Figure 2B). Instead, three positively charged residues, Arg18, Arg114, and His294, not present in the human enzyme and several water molecules provide interactions with Glu20, Thr183, Glu185, and Glu262, corresponding to human residues Glu15, Thr176, Glu178, and Glu256. Closest to the site opening is His294, the structural counterpart of human Phe285. The side chain of His294 interacts with a single water molecule that bridges to Oγ of Thr183 and, through another water molecule, to the NH1 nitrogen of Arg114, the second positively charged residue and the counterpart of human Phe111. On the basis of structural superpositions, the terminal nitrogen atoms of Arg114 occupy the same positions as the central carbon atoms of putrescine in the human structure. The Arg114 NH2 nitrogen atom interacts directly with Glu20 and indirectly, via two water molecules, with Glu185 and Arg18 (the analogue of Leu13 in human AdoMetDC). The guanidinium group of Arg18 is well anchored, forming one hydrogen bond each with a water molecule and Glu20 and two hydrogen bonds to Glu262. As the counterpart to human AdoMetDC Glu256, residue Glu262 in the potato enzyme initiates the hydrogen-bonding chain that links the charged

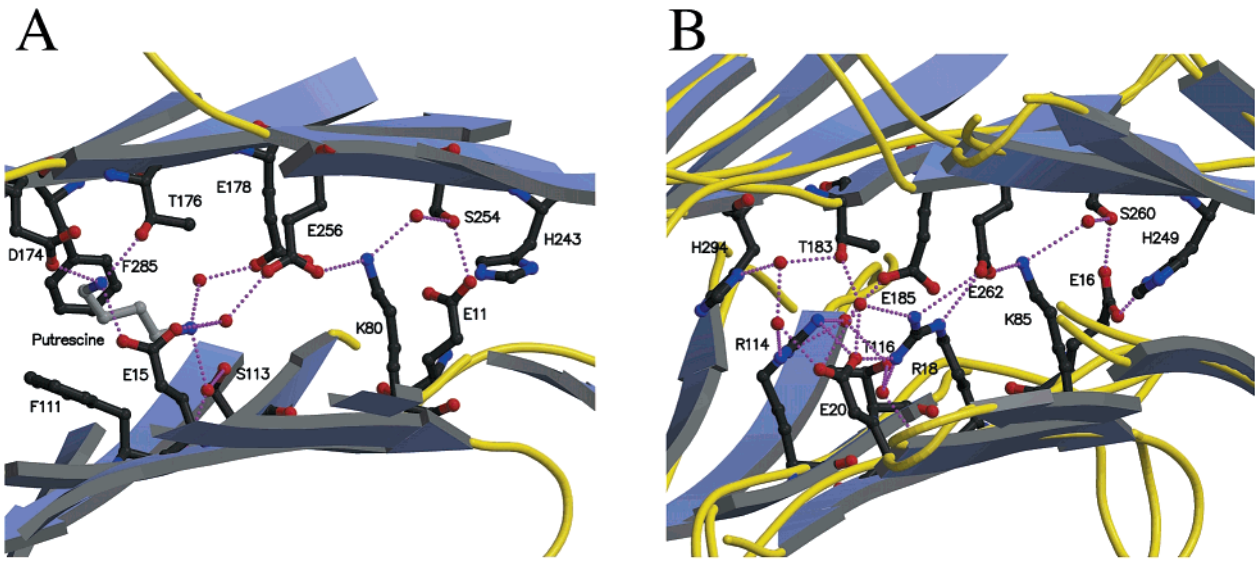

FIGURE 2: Comparison of the potato and human AdoMetDC buried charged site. (A) In the complex of human AdoMetDC with MAOEA (*32*), one end of putrescine is held in place by Asp174, Thr176, and Glu15. The hydrophobic center of putrescine packs against Phe111 and Phe285, while the other amino group makes water-mediated contacts with the protein. A chain of hydrogen bonds stretches from the putrescine to Glu11 in the active site. (B) No putrescine is observed bound to potato AdoMetDC. The substitutions Leu13/Arg18, Phe111/Arg114, Phe285/His294, and Asp174/Val181 alter the net charge in this region of the protein as compared to putrescine-free human AdoMetDC. Arg18 in the potato enzyme occupies the approximate position of putrescine in the human enzyme, making direct contact with Glu20 (counterpart of Glu15 in human AdoMetDC) and Glu262 (counterpart of Glu256 in human AdoMetDC). The hydrogen-bonding chain runs from Arg114 or His294 to His249 in the active site. Hydrogen bonds are shown as purple dotted lines and water molecules as red spheres. This figure was prepared with Molscript (*54*) and Raster3D (*55*).

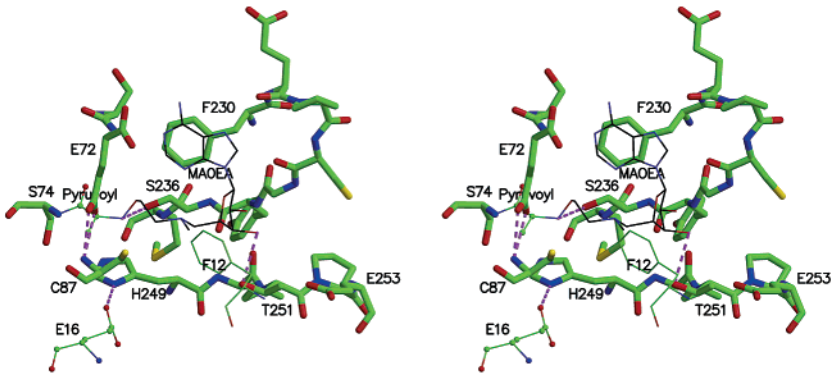

FIGURE 3: Stereoview of the potato AdoMetDC active site. Because no ligand was present in the active site and because the important residue Phe12 was disordered, the human AdoMetDC/MAOEA complex (*32*) was used to model the positions of Phe12 and suicide inhibitor MAOEA into the potato enzyme active site. Atoms in crystallographically determined positions are drawn as thick tubes, atoms in the crystal structure that were allowed to move during molecular mechanics modeling are drawn in ball-and-stick representation, and atoms based solely on modeling are shown as thin lines. Carbon atoms are shown in green (except MAOEA carbon atoms, shown in black), oxygen atoms are in red, nitrogen atoms are in blue, and the sulfur atoms are in yellow. This figure was prepared with Molscript (*54*) and Raster3D (*55*).

site and the active site. The chain involves Lys85 (Lys80 in the human enzyme), a conserved water molecule, Ser260, and Glu16 (Glu11 in the human enzyme). However, unlike the human enzyme, in the potato enzyme the chain continues, with Glu16 hydrogen bonding to the catalytically important residue His249 (His243 in the human enzyme).

Active Site. The crystal structure shows that the 40 kDa proenzyme has been fully processed into the 32 kDa α subunit and the 8 kDa β subunit. In the active site (Figure 3), the pyruvoyl group is clearly visible in the electron density. No substrate is present in the active site of the crystal, and the N-terminus, including the active site residue Phe12 (analogous to Phe7 in human AdoMetDC), is disordered. It is possible that some active site residues would become more ordered upon substrate binding. Side-chain conformations similar to those in human AdoMetDC/inhibitor structures (*32*) are observed for key residues such as Glu16, which plays a role in both autoprocessing and decarboxylation (*28*, *46*), Phe230, which stacks against the substrate purine base, and His249, which, based on data for the human enzyme (*46*), is believed to extract a proton from the α carbon of Ser73 during autoprocessing. Molecular mechanics modeling of the suicide inhibitor MAOEA and the potato N-terminus based on the human AdoMetDC/MAOEA complex predicts that Phe12 stacks against the MAOEA ribose, as in the human structure. The inhibitor itself adopts a conformation almost identical to that seen in the human structure (RMSD 0.45 Å after energy minimization).

In the computer model, some side chains in the active site adopt conformations different from those seen in the human structure. Cys87, believed to be the donor of the proton needed for product formation and release after decarboxylation (*47*), is observed pointing away from the modeled inhibitor. However, if upon substrate binding the side chain moves to adopt the most commonly observed cysteine rotamer, it will face the substrate with no backbone movement required. Glu253, which is expected to interact with the ribose 2′-OH and 3′-OH, adopts a crystallographic conformation pointing away from the modeled MAOEA. Adjustments to the side-chain and backbone torsion angles bring the side-chain carboxyl oxygens to within 3.4 Å of the ribose hydroxyl groups and also require an adjustment in the side chain of Thr251. The C-terminal residue of the β subunit, Glu72, is rotated approximately 180° around the backbone relative to the human enzyme, such that the side chain and terminal carboxylic acid have their positions reversed. The rotation allows the Glu72 side chain to make hydrogen bonds with Oγ of Thr90 and the backbone oxygen of Cys87 but does not appear to prevent the Cys87 side chain from reorienting to face the substrate.

DISCUSSION

Quaternary Structure. AdoMetDCs have been grouped into two classes on the basis of sequence alignment with AdoMetDCs from either lower organisms, such as *E. coli*, or higher organisms, such as humans. Plant enzymes and other enzymes assigned to the latter group were assumed to be dimeric (*6*). The present work shows that the potato enzyme differs from the other AdoMetDCs in the latter group in its quaternary structure. A comparison of the structures of human and potato enzymes explains why the potato AdoMetDC does not form a dimeric structure. The human enzyme dimer interface (Figure 4A) contains interactions from backbone atoms, water molecules, and side-chain/side-chain interactions involving residues Gln131 and Asn153, Tyr147 and Asp309, and Arg151 and Asp163 (*48*). In the potato enzyme, the Asn, Tyr, and Arg side chains are substituted by Val154, Ser158, and Asp160, respectively, and the loop from 157 to 164 (corresponding to human residues 150−156) contains a one-residue insertion, causing the loop to bulge. As shown in Figure 4B, a potato AdoMetDC dimer would be unlikely to form in the same manner as for the human enzyme, because in addition to the mutations, the bulge in the loop would create steric conflicts between the two monomers.

The biological relevance of dimerization remains unclear. The active site is located far from the dimer interface in the human structure, making it unlikely that catalysis is affected directly. However, as disrupting the dimer interface in human AdoMetDC would make the putrescine binding site more exposed, it is possible that intersubunit interactions are involved in regulation of AdoMetDC activity. The structure of the potato AdoMetDC suggests that it might be possible to convert the human AdoMetDC dimer to a monomer by

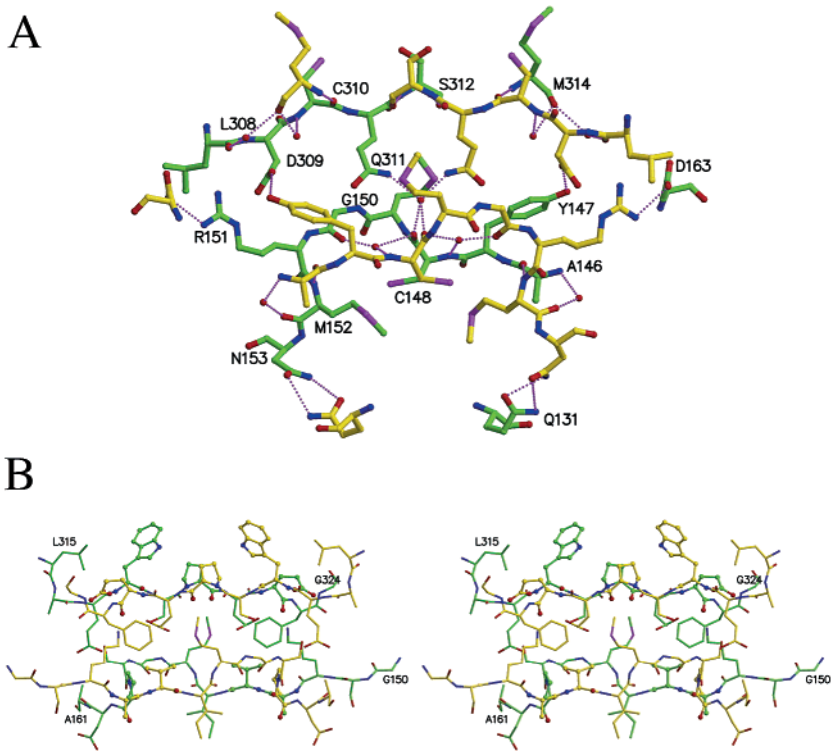

FIGURE 4: AdoMetDC quaternary structure. (A) Dimer interface in human AdoMetDC (*48*). One protomer has carbon atoms colored in green; the other has carbon atoms colored in yellow. Hydrogen bonds are indicated by purple dotted lines and water molecules by red spheres. Residue labels apply to the green monomer. (B) Stereoview of a hypothetical potato AdoMetDC dimer formed by superposition of two potato monomers on the human AdoMetDC/MAOEA complex dimer (*32*). One monomer has carbon atoms colored in green; the other has carbon atoms colored in yellow. A one-residue insertion in the potato enzyme causes a bulge in a loop (residues 157−164), generating steric conflicts between backbone atoms of the monomers (at bottom left and bottom right). The three side-chain-mediated dimerization contacts in the human structure are eliminated by the bulge and the substitutions Arg151/Ser158, Asn153/Asp160, and Tyr147/Val154. Residue labels apply to the green monomer. This figure was prepared with Molscript (*54*) and Raster3D (*55*).

mutating several residues to mimic the potato sequence. Studying such a mutated enzyme could shed light on the role of dimerization in regulation and putrescine activation.

Effects of C-Terminal Truncations. Xiong et al. previously showed that the potato enzyme tolerates C-terminal truncations up to but not including Thr335 (*7*). Thr335 does not directly interact with the active site; however, it is adjacent to Phe334. Phe334 is a central residue in a large group of buried hydrophobic side chains including Met188, Val277, Leu281, Phe289, Val291, and Leu315. It is likely that truncating Thr335 and inserting a terminal carboxyl group at Phe334 alters the positioning of the Phe334 side chain and disrupts proper folding of the enzyme.

Buried Charged Site. The structure of human AdoMetDC and sequence alignments suggest that all AdoMetDCs from higher organisms have an unusual site containing numerous buried charges (Figure 2). The site is located between the two central β-sheets. In the human enzyme, this site binds putrescine, which stimulates both the autocatalytic and decarboxylation reactions. Two mechanisms for stimulation have been previously proposed (*6*). By balancing the large number of negative charges in the site in the human enzyme, binding of putrescine might cause a shift in the relative orientations of the β-sheets. Such a change could be propagated to the active site, which is located at the opposite end of the β-sheets. No shift is observed in the potato AdoMetDC β-sheets relative to the human enzyme, nor would one be expected as both enzymes have only been observed crystallographically in the activated form. Alternatively, the human structure shows a hydrogen-bonding chain leading from the charged site to the active site (Figure 2A); the chain could be affected by putrescine binding and could affect the orientation of critical residues in the active site. The human structure shows the chain ending with Glu11, which has been implicated in both processing and decarboxylation (*49*).

The potato enzyme is not stimulated by putrescine but has basal levels of activity similar to putrescine-activated human AdoMetDC (*7*). The crystal structure provides a ready explanation for this behavior, as the substitutions Leu13/Arg18 and Phe111/Arg114 introduce two arginine residues into the buried charged site of the potato AdoMetDC. These residues probably play roles similar to putrescine by balancing charge and maintaining the hydrogen-bonding network that leads to the active site (Figure 2B). The central role of the two arginine residues was not predicted by examining the sequence alone, nor was it predicted by homology modeling (unpublished results). Indeed, as the corresponding residue Leu13 was not a key residue in the human enzyme, the possible contribution of Arg18 in plant AdoMetDCs was overlooked in the absence of the crystal structure.

Although the details of the buried charged site itself differ between the plant and human enzymes, the networks of hydrogen bonds leading between the charged site and the active site are nearly identical. The structure of the potato enzyme suggests that Glu16 makes a hydrogen-bonding contact with His249, which is believed to be responsible for abstraction of a proton from the α carbon of the catalytic

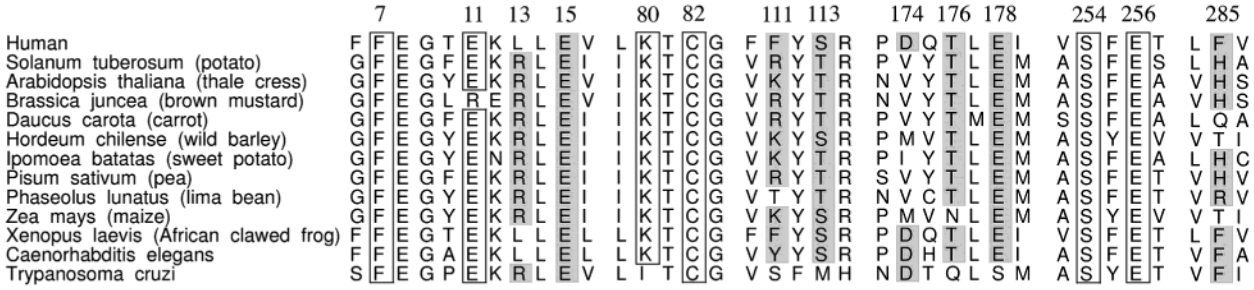

FIGURE 5: Alignment of AdoMetDC sequences. Residues in the active site and charged site are highly conserved across a variety of species, including mammals (human), amphibians (*X. laevis*), nematodes (*C. elegans*), protists (*T. cruzi*), and plants (the remaining sequences). Only key regions of the sequence are shown. Boxed and shaded residues can be expected to contribute to the activity of AdoMetDC; boxes indicate a residue in the active site, and shading indicates a residue in the charged site. Numbers are assigned on the basis of the human sequence. This figure was prepared with ClustalX (*56*) and Alscript (*57*).

serine during processing. In the human enzyme, the mutation E11D causes putrescine to have an inhibitory effect on processing, but other mutations in the charged site, such as D174E or E178D, can reverse that effect (*6*). The E11Q mutant processes at a slightly reduced rate that is not stimulated by putrescine and has low decarboxylation activity (*6*, *49*). The interaction between this residue and His249 in the potato structure, as well as the lack of an absolute requirement for the carboxylic acid functional group, suggests that the function of this residue in processing may be to properly position and activate the histidine side chain. Because the two arginine residues of potato AdoMetDC are a permanent part of the buried charged site, while putrescine binding in the human enzyme is reversible, the potato enzyme can be seen as always in the activated state.

Role of Lys85. Combined with the behavior of *Trypanosoma cruzi* AdoMetDC, which has the substitution Ile for Lys85 (Lys80 in human AdoMetDC) and for which processing is not stimulated by putrescine (unpublished observations), these results suggest that the hydrogen-bonding chain leading between the charged site and active site may be responsible for increasing the rate of processing. In the human enzyme, the mutation K80A abolishes putrescine simulation (*49*). By analogy, the mutation K85I or K85A might be expected to decrease the rapid rate of processing in the potato enzyme to levels similar to those seen for the human enzyme in the absence of putrescine. The proposal of a key processing activation role for Lys85 (Lys80 in human AdoMetDC) initially appears inconsistent with the behavior of *Neurospora crassa* AdoMetDC. Although this enzyme conserves the important residues in the charged site and the hydrogen-bonding chain, including Lys85, processing is not affected by putrescine and decarboxylation absolutely requires putrescine (*50*). However, this 503-residue enzyme is considerably larger than most other AdoMetDCs and on the basis of sequence alignments may have an altered structure in the region of the buried charged site possibly resulting in the participation of an additional glutamate residue. Interestingly, some parasite AdoMetDCs are similar to *N. crassa* in that (a) they also do not conserve Phe111 (Ser is present in *T. cruzi*, *Trypanosoma brucei*, and *Leishmania donovani*, while *Plasmodium falciparum* has Glu) and (b) the *T. cruzi* AdoMetDC decarboxylation reaction is stimulated by putrescine (*31*, *51*, *52*) even though processing is not. Putrescine stimulation of the processing reaction may therefore require both phenylalanine to properly orient the putrescine and lysine to transmit the effect of putrescine binding to the active site. However, the behavior of *T. cruzi* AdoMetDC suggests that the hydrogen-bonding chain does not explain putrescine stimulation of decarboxylation.

Properties of Parasitic AdoMetDCs. A phylogenetic tree analysis (not shown) leads to questions about AdoMetDCs from parasites, which diverge from the tree before the split between plants and animals. *T. cruzi*, *T. brucei*, and *L. donovani* AdoMetDCs contain a mix of charged site residues, having Asp174 and Phe285 in common with the human enzyme but Arg18 in common with plants. Amino acid residues at the positions in the parasitic enzymes corresponding to residues Lys80, Phe111, Thr176, and Glu178 in the charged site of human AdoMetDC are not conserved and are also different from the amino acid residues found at these positions in plant AdoMetDCs. It therefore seems unlikely that the charged site area in these enzymes functions in a manner directly comparable to plants or to animals. The bifunctional ornithine decarboxylase/AdoMetDC from *P. falciparum* has more key residues in common with mammalian AdoMetDCs, but it diverges from the tree sooner than other parasites and its decarboxylation reaction has been reported not to be stimulated by putrescine (*53*). Interestingly, although it shares Arg18 with plant enzymes, it does not conserve Ser260 (Ser 254 in human AdoMetDC). The effect of putrescine on autoprocessing of this enzyme has not been determined.

Our results show that the presence in the potato enzyme of several amino acid substitutions relative to human AdoMetDC provides side chains that mimic the role of putrescine. However, the putrescine stimulation of the *T. cruzi* AdoMetDC decarboxylation reaction suggests that the current understanding of activity regulation in AdoMetDC is incomplete and that structural determination of at least one of the parasitic AdoMetDC enzymes will be needed.

Comparison with Other Plant AdoMetDCs. The structure of potato AdoMetDC appears to be generally applicable to other plant AdoMetDCs. In particular, both the residues responsible for the monomeric quaternary structure of potato AdoMetDC and the arginine residues that replace putrescine in human AdoMetDC are highly conserved in plants. Among the 30 plant sequences examined from 23 species, only 2 sequences fail to conserve all of the key residues (see Figure 5 for a subset of the examined sequences). The *Brassica juncea* AdoMetDC lacks an equivalent to Glu16, instead having Arg at this position. However, *B. juncea* has two other AdoMetDC genes, both of which have the expected Glu in

this position. The published AdoMetDC sequence for *Triticum aestivum* has a Lys in place of Glu20. Because most of the putative plant AdoMetDCs have not been biochemically characterized, and because of the possibility of sequencing errors or inactive gene products, it is not possible to draw conclusions from these exceptions. The remaining 28 plant sequences have no mutations which would be expected to affect activity or disrupt the hydrogen-bonding scheme shown in Figure 2B. Several plants have changes at position His294, to either Gln or Thr. These residues could still participate in the hydrogen-bonding network but could not alter the net charge at the burried site relative to the human enzyme.

The analysis of plant sequence alignments also suggests that other plant enzymes are predominantly monomeric. All of the sequences examined contain the one-residue loop insertion seen in the potato enzyme, and several have a two-residue insertion. The side-chain/side-chain interactions that are present in the human enzyme but missing in the potato enzyme are also missing in other plant enzymes. Although many of the plant sequences conserve Tyr147 from the human sequence, its hydrogen-bonding partner Asp309 is missing in all examined plants, often being replaced by Ser, Thr, or Val. The Arg151/Asp163 interaction is not preserved, with Asp163 usually replaced by Ser or Thr and Arg151 replaced by either Gly or a variety of polar residues. Neither residue in the hydrogen-bonding pair Gln131/Asn153 is conserved in any of the plant sequences. The most common replacement is a Ser/Asp combination, but alanine is also frequently present in the second position. These changes to the dimer interface residues, and the variability in the residues replacing them, suggest that monomeric quaternary structure may be a common feature of plant AdoMetDCs. However, a smaller number of these residues are also changed in species more closely related to humans, including *Xenopus laevis* and *Caenorhabditis elegans*, whose AdoMetDC behaves as a dimer in gel filtration experiments (*29*).

ACKNOWLEDGMENT

We thank Dr. Sambit R. Kar for carrying out the ultracentrifugation studies. We also thank Ms. Leslie Kinsland for assistance in the preparation of the manuscript.

REFERENCES

1. Tabor, C. W., and Tabor, H. (1984) *Adv. Enzymol. Related Areas Mol. Biol. 56*, 251−282.
2. Pegg, A. E. (1986) *Biochem. J. 234*, 249−262.
3. Pegg, A. E., and McCann, P. P. (1992) *Pharmacol. Ther. 56*, 359−377.
4. van Poelje, P. D., and Snell, E. E. (1990) *Annu. Rev. Biochem. 59*, 29−59.
5. Hackert, M. L., and Pegg, A. E. (1997) in *Comprehensive Biological Catalysis* (Sinnott, M. L., Ed.) pp 201−216, Academic Press, London.
6. Ekstrom, J. L., Tolbert, W. D., Xiong, H., Pegg, A. E., and Ealick, S. E. (2001) *Biochemistry 40*, 9495−9504.
7. Xiong, H., Stanley, B. A., Tekwani, B. L., and Pegg, A. E. (1997) *J. Biol. Chem. 272*, 28342−28348.
8. Roberts, S. C., Scott, J., Gasteier, J. E., Jiang, Y., Brooks, B., Jardim, A., Carter, N. S., Heby, O., and Ullman, B. (2002) *J. Biol. Chem. 277*, 5902−5909.
9. Hoyt, M. A., Williams-Abbott, L. J., Pitkin, J. W., and Davis, R. H. (2000) *Mol. Gen. Genet. 263*, 664−673.
10. Müller, S., Da'daras, A., Lüersen, K., Wrenger, C., Gupta, R. D., Madhubala, R., and Walter, R. D. (2000) *J. Biol. Chem. 275*, 8097−8102.
11. Malmberg, R. L., Watson, M. B., Galloway, G. L., and Yu, W. (1998) *Crit. Rev. Plant Sci. 17*, 199−224.
12. Bagni, N., and Tassoni, A. (2001) *Amino Acids 20*, 301−317.
13. Galston, A. W., Kaursawhney, R., Altabella, T., and Tiburcio, A. F. (1997) *Bot. Acta 110*, 197−207.
14. Schröder, G., and Schröder, J. (1995) *Eur. J. Biochem. 228*, 74−78.
15. Lee, M. M., Lee, S. H., and Park, K. Y. (1997) *Plant Mol. Biol. 34*, 477−483.
16. Park, S.-J., and Cho, Y.-D. (1999) *J. Biochem. 126*, 996−1003.
17. Franceschetti, M., Hanfrey, C., Scaramagli, S., Torrigiani, P., Bagni, N., Burtin, D., and Michael, A. J. (2001) *Biochem. J. 353*, 403−309.
18. Raney, A., Law, G. L., Mize, G. J., and Morris, D. R. (2002) *J. Biol. Chem. 277*, 5988−5994.
19. Taylor, M. A., Mad Arif, S. A., Kumar, A., Davies, H. V., Scobie, L. A., Pearce, S. R., and Flavell, A. J. (1992) *Plant Mol. Biol. 20*, 641−651.
20. Song, J. J., Nada, K., and Tachibana, S. (2001) *Plant Sci. 161*, 507−515.
21. Yoshida, I., Yamagata, H., and Hirasawa, E. (1998) *J. Exp. Bot. 49*, 617−620.
22. Kumar, A., Altabella, T., Taylor, M. A., and Tiburcio, A. F. (1997) *Trends Plant Sci. 2*, 124−130.
23. Marco, F., and Carrasco, P. (2002) *Planta 214*, 641−647.
24. Pedros, A. R., MacLeod, M. R., Ross, H. A., McRae, D., Tiburcio, A. F., Davies, H. V., and Taylor, M. A. (1999) *Planta 209*, 153−160.
25. Kumar, A., Taylor, M. A., Mad Arif, S. A., and Davies, H. V. (1996) *Plant J. 9*, 147−158.
26. He, L., Nada, K., Kasukabe, Y., and Tachibana, S. (2002) *Plant Cell Physiol. 43*, 196−206.
27. Kameji, T., and Pegg, A. E. (1987) *Biochem. J. 243*, 285−288.
28. Stanley, B. A., Shantz, L. M., and Pegg, A. E. (1994) *J. Biol. Chem. 269*, 7901−7907.
29. Da'dara, A., and Walter, R. D. (1998) *Biochem. J. 336*, 545−550.
30. Da'dara, A. A., Henkle-Dührsen, K., and Walter, R. D. (1996) *Biochem. J. 320*, 519−530.
31. Kinch, L. N., and Phillips, M. A. (2000) *Biochemistry 39*, 3336−3343.
32. Tolbert, D. W., Ekstrom, J. L., Mathews, I. I., Secrist, J. A. I., Kapoor, P., Pegg, A. E., and Ealick, S. E. (2001) *Biochemistry 40*, 9484−9494.
33. Otwinowski, Z., and Minor, W. (1997) *Methods Enzymol. 276*, 307−326.
34. Brünger, A. T., Adams, P. D., Clore, G. M., DeLano, W. L., Gros, P., Grosse-Kunstleve, R. W., Jiang, J. S., Kuszewski, J., Nilges, M., Pannu, N. S., Read, R. J., Rice, L. M., Simonson, T., and Warren, G. L. (1998) *Acta Crystallogr. D 54*, 905−921.
35. Jones, T. A., Zou, J.-Y., Cowan, S. W., and Kjeldgaard, M. (1991) *Acta Crystallogr. A 47*, 110−119.
36. Martin, A. C. (1998) *ProFit V 1.8*, SciTech Software, London, England.
37. Jorgenson, W. L., Maxwell, D. S., and Tirado-Rives, J. (1996) *J. Am. Chem. Soc. 118*, 11225−11236.
38. Qiu, D., Shenkin, P. S., Hollinger, F. P., and Still, W. C. (1997) *J. Phys. Chem. A 101*, 3005−3014.
39. Ponder, J. W., and Richards, F. M. (1987) *J. Comput. Chem. 8*, 1016−1024.
40. Mohamadi, F., Richards, N. G. J., Guida, W. C., Liskamp, R., Lipton, M., Caufield, C., Chang, G., Hendrickson, T., and Still, W. C. (1990) *J. Comput. Chem. 11*, 460−467.
41. Fried, M. G., Kanugula, S., Bromberg, J. L., and Pegg, A. E. (1996) *Biochemistry 35*, 15295−15301.
42. Johnson, M. L., Correia, J. J., Yphantis, D. A., and Halvorson, H. R. (1981) *Biophys. J. 36*, 575−588.
43. Luzzati, P. V. (1952) *Acta Crystallogr. 5*, 802−810.
44. Ramachandran, G. N., and Sasisekharan, V. (1968) *Adv. Protein Chem. 23*, 283−437.
45. Laskowski, R. A., MacArthur, M. W., Moss, D. S., and Thornton, J. M. (1993) *J. Appl. Crystallogr. 26*, 283−291.
46. Xiong, H., and Pegg, A. E. (1999) *J. Biol. Chem. 274*, 35059−35066.
47. Xiong, H., Stanley, B. A., and Pegg, A. E. (1999) *Biochemistry 38*, 2462−2470.

48. Ekstrom, J. E., Matthews, I. I., Stanley, B. A., Pegg, A. E., and Ealick, S. E. (1999) *Structure 7*, 583−595.
49. Stanley, B. A., and Pegg, A. E. (1991) *J. Biol. Chem. 266*, 18502−18506.
50. Hoyt, M. A., Broun, M., and Davis, R. H. (2000) *Mol. Cell. Biol. 20*, 2760−2773.
51. Persson, K., Aslund, L., Grahn, B., Hanke, J., and Heby, O. (1998) *Biochem. J. 333*, 527−537.
52. Kinch, L. N., Scott, J. R., Ullman, B., and Phillips, M. A. (1999) *Mol. Biochem. Parasitol. 101*, 1−11.
53. Wrenger, C., Lüersen, K., Krause, T., Müller, S., and Walter, R. D. (2001) *J. Biol. Chem. 276*, 29651−29656.
54. Kraulis, P. J. (1991) *J. Appl. Crystallogr. 24*, 946−950.
55. Merritt, E. A., and Bacon, D. J. (1997) *Methods Enzymol. 277*, 505−524.
56. Thompson, J. D., Gibson, T. J., Plewniak, F., Jeanmougin, F., and Higgins, D. G. (1997) *Nucleic Acids Res. 24*, 4876−4882.
57. Barton, G. J. (1993) *Protein Eng. 6*, 37−40.

BI026710U